Journal of Experimental and Theoretical Physics, Vol. 96, No. 1, 2003, pp. 8–18.
Translated from Zhurnal Éksperimental'noĭ i Teoreticheskoĭ Fiziki, Vol. 123, No. 1, 2003, pp. 13–24.

NUCLEI, PARTICLES, AND THEIR INTERACTION

Magnetooptical Compression of Atomic Beams

V. I. Balykin and V. G. Minogin*

Institute of Spectroscopy, Russian Academy of Sciences, Troitsk, Moscow oblast, 142190 Russia
**e-mail: minogin@isan.troitsk.ru*

Received July 2, 2002

Abstract—We consider the propagation of an atomic beam in a quadrupole magnetic field under transverse irradiation by a cooling laser field. The cooling laser field was chosen in the form of a two-dimensional σ^+–σ^- configuration. We show that the sub-Doppler resonance in the radiation force can be used to reduce the diameter of the atomic beam to a value on the order of 10 μm. We establish that the simultaneous transverse cooling and compression of the atomic beam allow its phase density to be increased to values of the order of 10^{-4}–10^{-3}. The dipole interaction of an atom with the cooling and compressing laser field in a quadrupole magnetic field is analyzed in terms of a simple (3 + 5)-level model atom. © *2003 MAIK "Nauka/Interperiodica".*

1. INTRODUCTION

The compression of atomic beams to increase their phase density has been of considerable interest in recent years. One of the effective schemes is the compression of an atomic beam by a cooling laser field in a nonuniform magnetic field. Transverse cooling of an atomic beam in a potential well produced by a magnetic field causes the atomic oscillation amplitude in the potential and, accordingly, the atomic beam diameter to decrease. Previously, similar compression schemes were experimentally studied for transverse Doppler [1] and sub-Doppler [2] cooling of atomic beams. A deeper compression can be achieved in principle through a significant reduction in the beam temperature by using sub-Doppler cooling.

Attaining a high atomic beam phase density is of independent interest, because atomic beams are widely used in precision physical measurements, and of special interest in designing continuous-wave atomic lasers. The existing experimental schemes for attaining quantum degeneracy in atomic ensembles are known to be based on the evaporative cooling method [3, 4]. This cooling method can be applied to high-density atomic ensembles with a large number of atoms and with a low temperature. In all cases, the evaporative cooling method has been applied to laser-precooled atomic ensembles. All of the above three conditions in laser cooling of atoms are difficult to satisfy: low temperatures are reached at low atomic densities and, conversely, high densities prevent low temperatures from being reached. Despite these difficulties, the method has been effectively applied to atomic ensembles localized in magnetic or optical dipole traps. The long lifetime of the trapped atoms (on the order of 100 s) allows quantum degeneracy to be achieved even at a moderate initial phase density.

An atomic ensemble in the beam regime is of interest in that a continuous-wave atomic laser can be realized. However, quantum degeneracy in a beam is more difficult to achieve because of the limited preparation time of the atomic ensemble determined by the time of flight. Thus, for the evaporative cooling method to be applicable, the initial atomic phase density in the beams must be higher than that in the traps. Here, we consider a laser-cooling scheme that allows us to significantly increase the atomic beam phase density and, thereby, makes the subsequent evaporative cooling of the beam atoms possible to attain quantum degeneracy.

The effect of a magnetic field on the sub-Doppler cooling of atoms has previously been studied both theoretically [5–8] and experimentally [9, 10]. A magnetic field was used in experiments to extract atomic beams from magnetooptical traps [11–13]. The structure of the one-photon Doppler and two-photon sub-Doppler resonances in a magnetic field was investigated in [14, 15]. The multicomponent velocity distribution of the atomic cloud produced by the one- and two-photon resonances in a magnetooptical trap (MOT) was studied in [6, 7]. The authors of [6, 10] pointed out that under certain conditions, a magnetic field could even suppress the sub-Doppler cooling.

Here, our goal is to obtain analytical estimates for the maximum possible compression of an atomic beam in a nonuniform magnetic field and to estimate the atomic beam phase density reached in the case of transverse sub-Doppler cooling and compression.

We analyze the transverse compression of an atomic beam in a quadrupole axisymmetric magnetic field on which a cooling laser field was imposed. The laser field chosen as a two-dimensional σ^+–σ^- configuration produces transverse sub-Doppler cooling of the atomic beam, while the magnetic field produces a two-dimensional potential well across the atomic beam axis. The dipole interaction of the atoms with a nonuniform magnetic field and with a laser electric field is considered in a simple (3 + 5)-level model atom with the total

moments in the ground and excited states $F_g = 1$ and $F_e = 2$. In order that our results be applicable to real experimental schemes, the Lande g factors for the ground and excited states are assumed to be arbitrary. Our analysis reveals that the sub-Doppler resonances in the radiation force can be used for the simultaneous transverse cooling to sub-Doppler temperatures and the effective compression of the atomic beam to a diameter on the order of 10 μm.

2. THE COMPRESSION SCHEME AND THE MODEL ATOM

The scheme for transverse sub-Doppler compression of an atomic beam in a quadrupole magnetic field is shown in Fig. 1. In this scheme, four rectilinear currents I produce a magnetic field $\mathbf{B} = (B_x, B_y)$ near the electromagnetic quadrupole configuration axis whose components are defined by the standard relations [16]

$$B_y = -ay, \quad B_z = az. \tag{1}$$

Here, a is the magnetic field gradient on the quadrupole magnetic configuration axis, which depends on the currents I and on the distance R from the configuration axis to the currents.

The laser field was chosen in the form of two σ^+–σ^- configurations directed along the y and z axes. Each σ^+–σ^- configuration was composed of two counterpropagating, circularly polarized laser waves. In the coordinate system shown in Fig. 1, the electric field of the laser σ^+–σ^- configuration directed along the y axis is

$$\mathbf{E}^{(y)} = \frac{E_0}{2}[\mathbf{e}_+^y \exp(i(ky - \omega t)) - \mathbf{e}_-^y \exp(-i(ky - \omega t))] - \frac{E_0}{2}[\mathbf{e}_+^y \exp(i(ky + \omega t)) - \mathbf{e}_-^y \exp(-i(ky + \omega t))], \tag{2}$$

where

$$\mathbf{e}_\pm^y = \mp\frac{1}{\sqrt{2}}(\mathbf{e}_z \pm i\mathbf{e}_x)$$

are the unit circular vectors that correspond to the quantization y axis, $k = \omega/c$ is the magnitude of the wave vector, and ω is the laser field frequency. The first and second terms in Eq. (2) describe the waves with σ^+ and σ^- polarizations with respect to the quantization y axis, respectively. The electric field of the laser σ^+–σ^- configuration directed along the z axis in the coordinate system with the quantization z axis is

$$\mathbf{E}^{(z)} = \frac{E_0}{2}[\mathbf{e}_+^z \exp(i(kz - \omega t)) - \mathbf{e}_-^z \exp(-i(kz - \omega t))] - \frac{E_0}{2}[\mathbf{e}_+^z \exp(i(kz + \omega t)) - \mathbf{e}_-^z \exp(-i(kz + \omega t))], \tag{3}$$

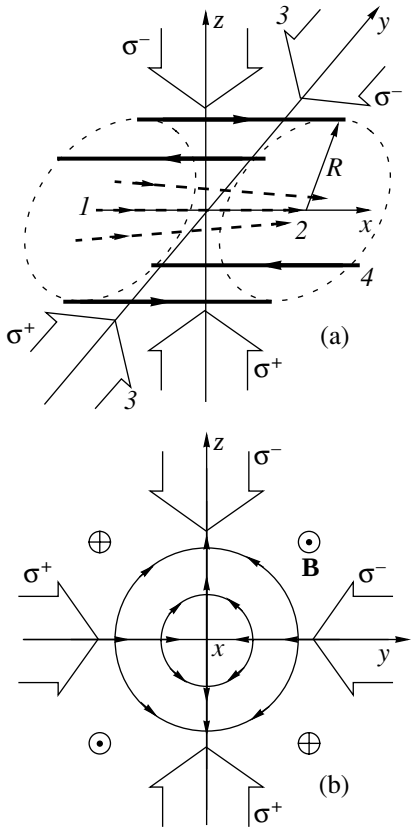

Fig. 1. (a) The scheme for laser sub-Doppler compression of an atomic beam in a quadrupole magnetic field: *1* incoming atomic beam, *2* outgoing atomic beam, *3* cooling laser beams, *4* electric currents producing a quadrupole magnetic field **B**. (b) The distribution of magnetic field **B** in the *yz* plane and the positions of the cooling laser beams.

where

$$\mathbf{e}_\pm^z = \mp\frac{1}{\sqrt{2}}(\mathbf{e}_x \pm i\mathbf{e}_y)$$

are the unit circular vectors that correspond to the quantization z axis. Similar to configuration (2), the first and second terms in Eq. (3) describe the waves with σ^+ and σ^- polarizations with respect to the quantization z axis, respectively.

Below, we estimate the basic parameters of the compressed atomic beam in a simple one-dimensional interaction model (see Fig. 2a). In this model, the atomic beam is compressed by the σ^+–σ^- configuration that propagates along the z axis. When the quantization z axis is chosen, this laser configuration induces the optical transitions in a (3 + 5)-level atom, shown in Fig. 2b. It should be immediately noted that all our estimates are also valid for the one-dimensional compression of the σ^+–σ^- configuration propagating along the y axis.

3. BASIC EQUATIONS

For the interaction scheme under consideration, the Hamiltonian can be written as

$$H = H_0 - \boldsymbol{\mu}\cdot\mathbf{B} - (\hbar^2/2M)\Delta - \mathbf{d}\cdot\mathbf{E}, \qquad (4)$$

where the Hamiltonian H_0 describes the quantized atomic states in the absence of a magnetic field and the second and last terms describe the dipole interaction of an atom with the nonuniform magnetic field $\mathbf{B} = B_z\mathbf{e}_z$ and with the laser field $\mathbf{E} = \mathbf{E}^{(z)}$, respectively.

A natural approach to describing the atomic motion in the chosen scheme is to use the atomic density matrix in the Wigner representation, $\rho = \rho(\mathbf{r}, \mathbf{p}, t)$. Below, we assume the density matrix $\rho_{\alpha\beta} = \langle\alpha|\rho|\beta\rangle$ to be determined from the time-independent eigenfunctions of the magnetic states α and $\beta = |F, m_F\rangle$. The energies E_{e_m} and E_{g_m} of the atomic Hamiltonian proper,

$$H_a = H_0 - \boldsymbol{\mu}\cdot\mathbf{B},$$

correspond to these eigenfunctions.

For a laser field composed of plane monochromatic traveling waves with a frequency ω close to the atomic transition frequencies $\omega_{mn} = (E_m - E_n)/\hbar$,

$$\mathbf{E} = \sum_a [\mathbf{E}^a \exp(i(\mathbf{k}_a\cdot\mathbf{r} - \omega t)) + \mathbf{E}^{a*}\exp(-i(\mathbf{k}_a\mathbf{r} - \omega t))], \qquad (5)$$

the equations of motion for the elements of the density matrix in Wigner representation and in the rotating-wave approximation can be written as [17, 18]

$$i\hbar\left(\frac{\partial}{\partial t} + \mathbf{v}\frac{\partial}{\partial\mathbf{r}}\right)\rho_{kl}(\mathbf{r}, \mathbf{p}) = (E_k - E_l)\rho_{kl}(\mathbf{r}, \mathbf{p})$$

$$- \sum_{a, m}(\mathbf{d}_{km}\cdot\mathbf{E}^a)\rho_{ml}\left(\mathbf{r}, \mathbf{p} - \frac{1}{2}\hbar\mathbf{k}_a\right)\exp(i\mathbf{k}_a\cdot\mathbf{r} - i\omega t)$$

$$+ \sum_{a, n}(\mathbf{d}_{nl}\cdot\mathbf{E}^a)\rho_{kn}\left(\mathbf{r}, \mathbf{p} + \frac{1}{2}\hbar\mathbf{k}_a\right)\exp(i\mathbf{k}_a\cdot\mathbf{r} - i\omega t)$$

$$- \sum_{a, m}(\mathbf{d}_{km}\cdot\mathbf{E}^{a*})\rho_{ml}\left(\mathbf{r}, \mathbf{p} + \frac{1}{2}\hbar\mathbf{k}_a\right)\exp(-i\mathbf{k}_a\cdot\mathbf{r} + i\omega t) \qquad (6)$$

$$+ \sum_{a, n}(\mathbf{d}_{nl}\cdot\mathbf{E}^{a*})\rho_{kn}\left(\mathbf{r}, \mathbf{p} - \frac{1}{2}\hbar\mathbf{k}_a\right)\exp(-i\mathbf{k}_a\cdot\mathbf{r} + i\omega t)$$

$$+ i\hbar\langle k|\Gamma\rho(\mathbf{r}, \mathbf{p})|l\rangle,$$

where $\mathbf{d}_{kl} = \langle k|d|l\rangle$ are the matrix elements of the atomic dipole moment operator. All four sums in Eqs. (6) are assumed to include terms that correspond only to positive atomic frequencies,

$$\omega_{pq} = \frac{E_p - E_q}{\hbar} > 0.$$

The first, second, third, and fourth sums include, respectively, the terms with frequencies

$$\omega_{km} = \frac{E_k - E_m}{\hbar} > 0,$$

$$\omega_{nl} = \frac{E_n - E_l}{\hbar} > 0,$$

$$\omega_{mk} = \frac{E_m - E_k}{\hbar} > 0,$$

$$\omega_{ln} = \frac{E_l - E_n}{\hbar} > 0.$$

The first term in Eqs. (6) describes the contributions from the radiative relaxation operator Γ.

Note that in Eqs. (6), we omitted the small magnetodipole forces

$$\mathbf{f}_\alpha = \partial\langle\alpha|\boldsymbol{\mu}\cdot\mathbf{B}|\alpha\rangle/\partial\mathbf{r},$$

which play no significant role in the dynamics of the atom.

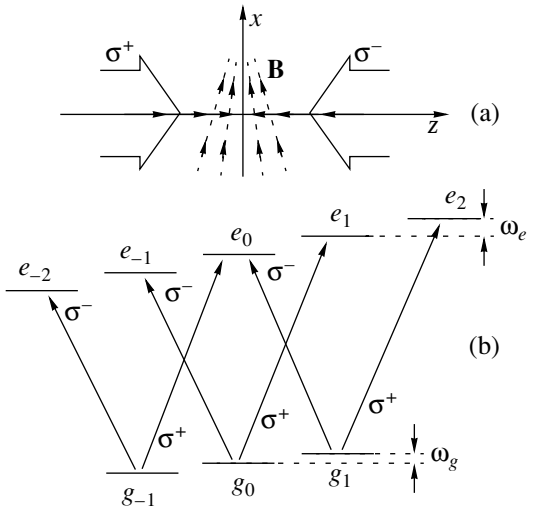

Fig. 2. (a) The one-dimensional compression of an atomic beam in the field of the laser σ^+–σ^- configuration propagating along the z axis. The magnetic field is directed along the z axis and the atomic beam propagates along the x axis. (b) Zeeman energy levels for the (3 + 5)-level atom in the coordinate system with the quantization z axis for positive Zeeman shifts, $\omega_g > 0$ and $\omega_e > 0$. The arrows indicate the transitions induced by the $\sigma^\pm$- and π-polarized laser waves.

Below, the Zeeman shifts of the magnetic states are considered in the simplest linear approximation in magnetic field strength. For the ground-state sublevels,

$$\langle F_g, m_g|-\boldsymbol{\mu}\cdot\mathbf{B}|F_g, m_g\rangle = \mu_B g_g B_z m_g; \qquad (7)$$

for the excited-state sublevels,

$$\langle F_e, m_e|-\boldsymbol{\mu}\cdot\mathbf{B}|F_e, m_e\rangle = \mu_B g_e B_z m_e. \qquad (8)$$

Here, μ_B is the Bohr magneton; g_g and g_e are the Lande g factors for the ground and excited states, respectively; $F_g = 1$, $m_g = -1, 0, 1$; $F_e = 2$, $m_e = -2, -1, 0, 1, 2$.

Below, we give Eqs. (6) for a (3 + 5)-level atom in explicit form in the practically important case of weakly saturated atomic transitions. In this case, it will suffice to take into consideration the equations only for the diagonal elements of the density matrix, for the nondiagonal one-photon elements describing optical coherences, and for one nondiagonal two-photon element describing the coherence between the sublevels g_{-1} and g_1 of the ground state g. Concurrently, we eliminate the explicit dependence on time and coordinate from the equations by the following simple substitutions:

$$\begin{aligned}
\rho_{g_{-1}e_{-2}} &= \sigma_{g_{-1}e_{-2}}\exp(i\omega t + ikz),\\
\rho_{g_{-1}e_0} &= \sigma_{g_{-1}e_0}\exp(i\omega t - ikz),\\
\rho_{g_0e_{-1}} &= \sigma_{g_0e_{-1}}\exp(i\omega t + ikz),\\
\rho_{g_0e_1} &= \sigma_{g_0e_1}\exp(i\omega t - ikz),\\
\rho_{g_1e_0} &= \sigma_{g_1e_0}\exp(i\omega t + ikz),\\
\rho_{g_1e_2} &= \sigma_{g_1e_2}\exp(i\omega t - ikz),\\
\rho_{g_{-1}g_1} &= \sigma_{g_{-1}g_1}\exp(-2ikz).
\end{aligned}$$

After these substitutions, the equations for the atomic density matrix elements that describe the dipole interaction of the (3 + 5)-level atom with the laser field $\mathbf{E} = \mathbf{E}^{(z)}$ in a nonuniform magnetic field $\mathbf{B} = B_z\mathbf{e}_z$ in the approximation of weak saturation are

$$\begin{aligned}
\frac{d}{dt}\rho_{g_{-1}g_{-1}} &= i\Omega(\sigma^{(-)}_{e_{-2}g_{-1}} - \sigma^{(-)}_{g_{-1}e_{-2}}) + \frac{i\Omega}{\sqrt{6}}(\sigma^{(+)}_{e_0g_{-1}} - \sigma^{(+)}_{g_{-1}e_0})\\
&+ \gamma\int\left(2\Phi_\sigma(\mathbf{n})\rho^{(\mathbf{n})}_{e_{-2}e_{-2}} + \Phi_\pi(\mathbf{n})\rho^{(\mathbf{n})}_{e_{-1}e_{-1}} + \frac{1}{3}\Phi_\sigma(\mathbf{n})\rho^{(\mathbf{n})}_{e_0e_0}\right)d^2n,\\
\frac{d}{dt}\rho_{g_0g_0} &= \frac{i\Omega}{\sqrt{2}}(\sigma^{(-)}_{e_{-1}g_0} - \sigma^{(-)}_{g_0e_{-1}} + \sigma^{(+)}_{e_1g_0} - \sigma^{(+)}_{g_0e_1})\\
&+ \gamma\int\left(\Phi_\sigma(\mathbf{n})\rho^{(\mathbf{n})}_{e_{-1}e_{-1}} + \frac{4}{3}\Phi_\pi(\mathbf{n})\rho^{(\mathbf{n})}_{e_0e_0} + \Phi_\sigma(\mathbf{n})\rho^{(\mathbf{n})}_{e_1e_1}\right)d^2n,\\
\frac{d}{dt}\rho_{g_1g_1} &= i\Omega(\sigma^{(+)}_{e_2g_1} - \sigma^{(+)}_{g_1e_2}) + \frac{i\Omega}{\sqrt{6}}(\sigma^{(-)}_{e_0g_1} - \sigma^{(-)}_{g_1e_0})\\
&+ \gamma\int\left(\frac{1}{3}\Phi_\sigma(\mathbf{n})\rho^{(\mathbf{n})}_{e_0e_0} + \Phi_\pi(\mathbf{n})\rho^{(\mathbf{n})}_{e_1e_1} + 2\Phi_\sigma(\mathbf{n})\rho^{(\mathbf{n})}_{e_2e_2}\right)d^2n,\\
\frac{d}{dt}\rho_{e_{-2}e_{-2}} &= i\Omega(\sigma^{(+)}_{g_{-1}e_{-2}} - \sigma^{(+)}_{e_{-2}g_{-1}}) - 2\gamma\rho_{e_{-2}e_{-2}},\\
\frac{d}{dt}\rho_{e_{-1}e_{-1}} &= \frac{i\Omega}{\sqrt{2}}(\sigma^{(+)}_{g_0e_{-1}} - \sigma^{(+)}_{e_{-1}g_0}) - 2\gamma\rho_{e_{-1}e_{-1}},\\
\frac{d}{dt}\rho_{e_0e_0} &= \frac{i\Omega}{\sqrt{6}}(\sigma^{(-)}_{g_{-1}e_0} - \sigma^{(-)}_{e_0g_{-1}} + \rho^{(+)}_{g_1e_0} - \rho^{(+)}_{e_0g_1}) - 2\gamma\rho_{e_0e_0},\\
\frac{d}{dt}\rho_{e_1e_1} &= \frac{i\Omega}{\sqrt{2}}(\sigma^{(-)}_{g_0e_1} - \sigma^{(-)}_{e_1g_0}) - 2\gamma\rho_{e_1e_1},\\
\frac{d}{dt}\rho_{e_2e_2} &= i\Omega(\sigma^{(-)}_{g_1e_2} - \sigma^{(-)}_{e_2g_1}) - 2\gamma\rho_{e_2e_2},\\
\frac{d}{dt}\sigma_{g_{-1}e_{-2}} &= i\Omega(\rho^{(-)}_{e_{-2}e_{-2}} - \rho^{(+)}_{g_{-1}g_{-1}})\\
&- (\gamma - i(\omega_g - 2\omega_e - \delta_1))\sigma_{g_{-1}e_{-2}},\\
\frac{d}{dt}\sigma_{g_{-1}e_0} &= -\frac{i\Omega}{\sqrt{6}}(\rho^{(-)}_{g_{-1}g_{-1}} + \sigma^{(+)}_{g_{-1}g_1} - \rho^{(+)}_{e_0e_0})\\
&- (\gamma - i(\omega_g - \delta_{-1}))\sigma_{g_{-1}e_0},\\
\frac{d}{dt}\sigma_{g_0e_{-1}} &= -\frac{i\Omega}{\sqrt{2}}(\rho^{(+)}_{g_0g_0} - \rho^{(-)}_{e_{-1}e_{-1}}) - (\gamma + i(\omega_e + \delta_1))\sigma_{g_0e_{-1}},\\
\frac{d}{dt}\sigma_{g_0e_1} &= -\frac{i\Omega}{\sqrt{2}}(\rho^{(-)}_{g_0g_0} - \rho^{(-)}_{e_{-1}e_{-1}}) - (\gamma - i(\omega_e - \delta_{-1}))\sigma_{g_0e_1},\\
\frac{d}{dt}\sigma_{g_1e_0} &= -\frac{i\Omega}{\sqrt{6}}(\rho^{(+)}_{g_1g_1} + \sigma^{(-)}_{g_1g_{-1}} - \rho^{(-)}_{e_0e_0})\\
&- (\gamma + i(\omega_g + \delta_1))\sigma_{g_1e_0},\\
\frac{d}{dt}\sigma_{g_1e_2} &= -i\Omega(\rho^{(-)}_{g_1g_1} - \rho^{(+)}_{e_2e_2})\\
&- (\gamma + i(\omega_g - 2\omega_e + \delta_{-1}))\sigma_{g_1e_2},\\
\frac{d}{dt}\sigma_{g_{-1}g_1} &= \frac{i\Omega}{\sqrt{6}}(\sigma^{(+)}_{e_0g_1} - \sigma^{(-)}_{g_{-1}e_0}) + 2i(\omega_g + kv)\sigma_{g_{-1}g_1}.
\end{aligned} \qquad (9)$$

Above, we use the following notation for the density matrix elements:

$$\rho_{ab} = \langle a|\rho(\mathbf{r}, \mathbf{p}, t)|b\rangle,$$

$$\rho_{ab}^{(\pm)} = \left\langle a\left|\rho\left(\mathbf{r}, \mathbf{p} \pm \frac{1}{2}\hbar\mathbf{k}, t\right)\right|b\right\rangle,$$

$$\rho_{ab}^{(\mathbf{n})} = \langle a|\rho(\mathbf{r}, \mathbf{p} + \mathbf{n}\hbar k, t)|b\rangle,$$

where $\mathbf{k} = k\mathbf{e}_z$ and $\mathbf{n}$ is the unit vector that specifies the direction of the spontaneous photon emission. The total time derivative is

$$\frac{d}{dt} = \frac{\partial}{\partial t} + v\frac{\partial}{\partial \mathbf{r}}. \tag{10}$$

The Rabi frequency Ω and the spontaneous decay rate of the upper magnetic sublevels 2γ are defined as

$$\Omega = \frac{\|d\|E_0}{2\sqrt{5}\hbar}, \quad 2\gamma = W_{sp} = \frac{4}{3}\frac{\|d\|^2\omega_0^3}{\hbar c^3}, \tag{11}$$

where $\|d\|$ is the reduced matrix element. The main, δ, and two Doppler-shifted, $\delta_{\pm 1}$, detunings are given by the relations

$$\delta = \omega - \omega_0, \quad \delta_{\pm 1} = \omega - \omega_0 \pm kv, \tag{12}$$

where $v = v_z$ is the velocity component along the z axis. The frequencies

$$\omega_g = \mu_B g_g a z/\hbar, \quad \omega_e = \mu_B g_e a z/\hbar \tag{13}$$

define the Zeeman shifts of the magnetic sublevels, which depend on the atom coordinate and which can have any signs. The functions $\Phi_\sigma(\mathbf{n})$ and $\Phi_\pi(\mathbf{n})$ define the angular anisotropy in spontaneous emission:

$$\Phi_\sigma(\mathbf{n}) = \frac{3}{16\pi}(1 + n_z^2), \quad \Phi_\pi(\mathbf{n}) = \frac{3}{8\pi}(1 - n_z^2), \tag{14}$$

where $n_z = \cos\theta$ is the component of the unit vector $\mathbf{n}$ along the quantization z axis. The integration in the radiation arrival terms is performed over the directions of spontaneous emission specified by the unit vector $\mathbf{n}$, $d^2n = \sin\theta d\theta d\phi$.

4. THE KINETIC EQUATION

The difference differential equations (9), which do not include the explicit dependence on time and coordinate, can be analyzed in a standard way [19]. If the atom–field interaction time is much longer than the spontaneous decay time, $\tau_{\text{int}} \gg \tau_{sp} = 1/2\gamma$, then the momentum width of the density matrix elements can be assumed to exceed the photon momentum $\hbar k$. This assumption, which always holds below, allows the atomic density matrix elements to be expanded in terms of powers of the photon momentum $\hbar k$. Considering below the equations expanded in terms of sequentially increasing orders of the photon momentum $\hbar k$, we can infer that the diagonal (ρ_{aa}) and nondiagonal (σ_{ab}) density matrix elements are the functionals of the Wigner distribution function $w(\mathbf{r}, \mathbf{p}, t)$,

$$w = \sum \rho_{g_\alpha g_\alpha} + \left(\sum \rho_{e_\beta e_\beta}\right), \tag{15}$$

where $\alpha = -1, 0, 1$ and $\beta = -2, -1, 0, 1, 2$.

The general structure of the functional dependence can be directly determined from the structure of the expanded equations:

$$\begin{aligned}
\rho_{aa} &= \left(R_{aa}^0 + \frac{1}{2}\hbar k R_{aa}^1 + \ldots\right)w \\
&\quad + \frac{1}{2}\hbar k(Q_{aa}^1 + \ldots)\frac{\partial w}{\partial p_z} + \ldots, \\
\sigma_{ab} &= \left(S_{ab}^0 + \frac{1}{2}\hbar k S_{ab}^1 + \ldots\right)w \\
&\quad + \frac{1}{2}\hbar k(T_{ab}^1 + \ldots)\frac{\partial w}{\partial p_z} + \ldots,
\end{aligned} \tag{16}$$

where R_{aa}^0, R_{aa}^1, Q_{aa}^1, …, S_{ab}^0, S_{ab}^1, T_{ab}^1, … are the functions of momentum $\mathbf{p}$ (or velocity $\mathbf{v} = \mathbf{p}/M$), which are determined by the solution procedure. By the definition of the distribution function (15), the unknown diagonal functions satisfy the normalization conditions

$$\sum R_{g_\alpha g_\alpha}^0 + R_{e_\beta e_\beta}^0 = 1, \tag{17}$$

$$\sum R_{g_\alpha g_\alpha}^1 + R_{e_\beta e_\beta}^1 = 0, \tag{18}$$

$$\sum Q_{g_\alpha g_\alpha}^1 + Q_{e_\beta e_\beta}^1 = 0. \tag{19}$$

Taking into account the structure of solution (16), we can see from the expanded equations that the Wigner function $w(\mathbf{r}, \mathbf{p}, t)$ satisfies the closed equation. To within the second order in photon momentum $\hbar k$, the closed equation for the distribution function is the Fokker–Planck equation:

$$\frac{\partial w}{\partial t} + \mathbf{v}\frac{\partial w}{\partial \mathbf{r}} = -\frac{\partial}{\partial p_z}(Fw) + \sum \frac{\partial^2}{\partial p_i^2}(D_{ii}w), \tag{20}$$

where $i = x, y, z$. The kinetic coefficients F and D_{ii} in Eq. (20) define the radiation force and the momentum diffusion tensor:

$$\begin{aligned}
F &= \hbar k\Omega\left[i(S_{g_1e_2}^0 - S_{e_2g_1}^0 + S_{e_{-2}g_{-1}}^0 - S_{g_{-1}e_{-2}}^0)\right. \\
&\quad + \frac{i}{\sqrt{2}}(S_{g_0e_1}^0 - S_{e_1g_0}^0 + S_{e_{-1}g_0}^0 - S_{g_0e_{-1}}^0) \\
&\quad \left. + \frac{i}{\sqrt{6}}(S_{g_{-1}e_0}^0 - S_{e_0g_{-1}}^0 + S_{e_0g_1}^0 - S_{g_1e_0}^0)\right],
\end{aligned} \tag{21}$$

$$
\begin{aligned}
D_{ii} &= \hbar^2 k^2 \gamma \\
&\times \Big[\alpha_{ii}^{\sigma} \Big(R^0_{e_{-2}e_{-2}} + \frac{1}{2} R^0_{e_{-1}e_{-1}} + \frac{1}{3} R^0_{e_0 e_0} + \frac{1}{2} R^0_{e_1 e_1} + R^0_{e_2 e_2} \Big) \\
&\quad + \alpha_{ii}^{\pi} \Big(\frac{1}{2} R^0_{e_{-1}e_{-1}} + \frac{2}{3} R^0_{e_0 e_0} + \frac{1}{2} R^0_{e_1 e_1} \Big) \Big] \\
&+ \frac{1}{2} \delta_{iz} \hbar^2 k^2 \Omega \Big[i (T^1_{g_{-1}e_{-2}} - T^1_{e_{-2}g_{-1}} + T^1_{e_2 g_1} - T^1_{g_1 e_2}) \\
&\quad + \frac{i}{\sqrt{2}} (T^1_{g_0 e_{-1}} - T^1_{e_{-1}g_0} + T^1_{e_1 g_0} - T^1_{g_0 e_1}) \\
&\quad + \frac{i}{\sqrt{6}} (T^1_{e_0 g_{-1}} - T^1_{g_{-1}e_0} + T^1_{g_1 e_0} - T^1_{e_0 g_1}) \Big].
\end{aligned}
\tag{22}
$$

In these equations, the coefficients α_{ii}^{σ} and α_{ii}^{π} take into account the angular anisotropy in spontaneous photon emission,

$$
\alpha_{ii}^{\sigma} = \int \Phi_{\sigma}(\mathbf{n}) n_i^2 d^2 n, \quad \alpha_{ii}^{\pi} = \int \Phi_{\pi}(\mathbf{n}) n_i^2 d^2 n. \tag{23}
$$

In explicit form, the angular anisotropy coefficients are

$$
\begin{aligned}
\alpha_{xx}^{\sigma} &= \alpha_{yy}^{\sigma} = \frac{3}{10}, \quad \alpha_{zz}^{\sigma} = \frac{2}{5}, \\
\alpha_{xx}^{\pi} &= \alpha_{yy}^{\pi} = \frac{2}{5}, \quad \alpha_{zz}^{\pi} = \frac{1}{5}.
\end{aligned}
\tag{24}
$$

The force F and the diffusion tensor D_{ii} can be explicitly determined from the solution of the steady-state equations that follow from the expanded equations for the atomic density matrix elements considered separately in the zero and first orders in photon momentum $\hbar k$. The steady-state equations for the functions R^0_{aa} and S^0_{ab}, as well as for Q^1_{aa} and T^1_{ab} in the case of weakly saturated transitions, are given in Appendices A and B.

5. FORCES ACTING ON AN ATOM

The radiation force that acts on an atom in the scheme under consideration depends both on the velocity and on the coordinate of the atom. In the approximation of weak saturation, the one-photon optical processes described by the coherences between the sublevels g_α and $e_{\alpha \pm 1}$ and the two-photon processes described by the coherences between the ground-state sublevels g_{-1} and g_1 contribute to the force.

Below, we consider the radiation force in the practically important case of large negative detunings ($-\delta \gg \gamma$), where the radiation force produces the deepest sub-Doppler cooling of an atomic beam [20, 21]. Restricting our analysis to low velocities ($kv \ll \gamma$) and small Zeeman shifts ($|\omega_g|, |\omega_e| \ll \gamma$), we can derive the following approximate expression for the radiation force near the axis of the compressing configuration ($z = 0$), which reduces to the sum of the forces due to one- and two-photon processes (Fig. 3):

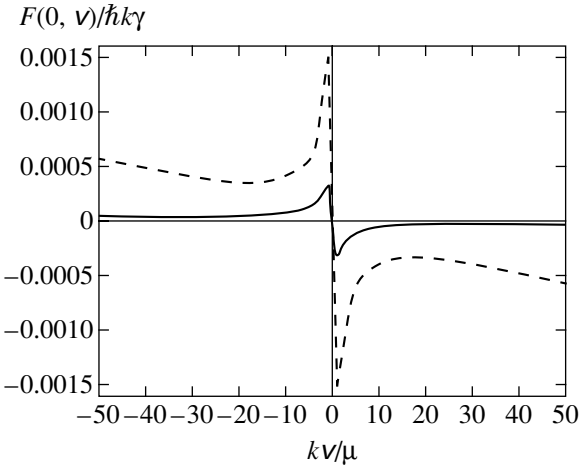

Fig. 3. Radiation force versus velocity at $z = 0$, the detuning $\delta = -10\gamma$, and the saturation parameter $G = 0.1$ (solid line) and 0.5 (dashed line). The sub-Doppler resonance line halfwidths $\mu = 0.18\gamma$ (solid line) and 0.90γ (dashed line) correspond to the chosen detuning and saturation parameter.

$$
\begin{aligned}
F(0, v) &= -\frac{25}{11} \hbar k \gamma \frac{G\gamma^2}{\delta^2} \frac{(88/85) + (kv/\mu)^2}{1 + (kv/\mu)^2} \frac{kv}{|\delta|} \\
&\quad - \frac{60}{17} \hbar k \gamma \frac{kv/|\delta|}{1 + (kv/\mu)^2},
\end{aligned}
\tag{25}
$$

where

$$
G = \frac{2\Omega^2}{\gamma^2} = \frac{1}{10} \Big(\frac{\|d\| E_0}{\hbar \gamma} \Big)^2 \tag{26}
$$

is the dimensionless saturation parameter and

$$
\mu = \frac{1}{4} \sqrt{\frac{17}{33}} \frac{G\gamma^2}{|\delta|} = \frac{1}{2} \sqrt{\frac{17}{33}} \frac{\Omega^2}{|\delta|} \tag{27}
$$

is the sub-Doppler resonance halfwidth for $|\delta| \gg \gamma$.

Under the same conditions, the force acting on a static atom is also the sum of the forces due to one- and two-photon processes (Fig. 4):

$$
\begin{aligned}
F(z, 0) &= -\frac{5}{11} \hbar k \gamma \frac{G\gamma^2}{|\delta|^3} \\
&\times \frac{(44/17)(3\omega_e - \omega_g) + (8\omega_e - 3\omega_g)(\omega_g/\mu)^2}{1 + (\omega_g/\mu)^2} \\
&\quad - \frac{60}{17} \hbar k \gamma \frac{\omega_g/|\delta|}{1 + (\omega_g/\mu)^2}.
\end{aligned}
\tag{28}
$$

Recall that the Zeeman shifts ω_g and ω_e are proportional to the z coordinate.

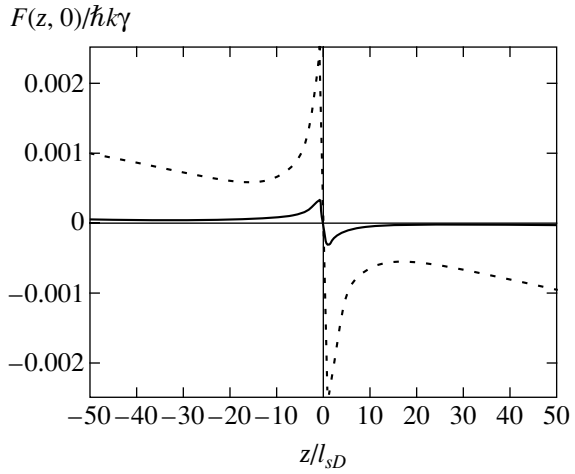

Fig. 4. Radiation force versus coordinate at a zero velocity, the detuning $\delta = -10\gamma$, and the saturation parameter $G = 0.1$ (solid line) and 0.5 (dotted line) for the Lande factors $g_g = 1/3$ and $g_e = 1/2$. The value of l_{sD} defined by (30) was chosen as the scale length.

The broad parts of the velocity and coordinate dependences of the radiation force are attributable to the one-photon absorption (emission) weakly perturbed by two-photon processes. In our case of large detunings ($|\delta| \gg \gamma \gg \mu$), the broad velocity dependence originates from the two resonances of one-photon absorption (emission) located at the velocities $kv_{\text{res}} = \pm\delta$. The broad spatial dependence of the radiation force originates from the one-photon resonances related to the Zeeman shift frequencies.

The narrow resonances in the field are attributable to two-photon processes. For an atom that moves in a zero magnetic field, i.e., at $z = 0$, the two-photon processes are effective at two-photon resonance velocities

$$(\omega \pm kv) - (\omega \mp kv) \approx 0,$$

i.e., at velocities $v \approx 0$. For a static atom ($v = 0$), the two-photon processes are effective for

$$(\omega \pm \omega_g) - (\omega \mp \omega_g) \approx 0,$$

i.e., for $\omega_g \approx 0$ or for $z \approx 0$ (Fig. 4).

The characteristic velocity scale of the change in the force due to the sub-Doppler resonance is determined by the characteristic velocity $v_{sD} = \mu/k$, which for weak saturation and for a large negative detuning is

$$v_{sD} = \frac{1}{4}\sqrt{\frac{17}{33}}\frac{G\gamma\gamma}{|\delta|}\frac{\gamma}{k}. \tag{29}$$

The characteristic spatial scale of the change in the force due to the sub-Doppler resonance is determined by the length l_{sD} on which the Zeeman ground-state sublevel splitting is equal to the two-photon resonance width. For weak saturation and for a large negative detuning, the condition $\omega_g = \mu$ specifies the scale length

$$l_{sD} = \frac{\hbar\mu}{\mu_B g_g a}. \tag{30}$$

For definiteness, we estimate the degree of beam compression for ^{85}Rb atoms that interact with laser radiation on the $5^2S_{1/2}(F = 3) - 5^2P_{3/2}(F = 4)$ dipole transition at the wavelength $\lambda = 780$ nm. In general, this scheme is described by a (7 + 9)-level model atom. However, since the higher order multiphoton processes give small contributions to the radiation force, a simple (3 + 5)-level model can be used to estimate the main effects. For the optical transition under consideration, $g_g = 1/3$ and $g_e = 1/2$. If, for example, we choose the saturation parameter $G = 0.5$ and the detuning $d = -10\gamma$, then the characteristic velocity interval is $v_{sD} = 2.1$ cm s^{-1}. For a moderate magnetic field gradient, $a = 10$ G cm^{-1}, the characteristic spatial scale is $l_{sD} = 50$ μm.

6. BEAM COMPRESSION

The radiation force (28) produces a potential well across the atomic beam axis:

$$U(z) = -\int F(z, 0)dz.$$

For large detunings ($|\delta| \gg \gamma$) and for the Lande factors $g_g = 1/3$ and $g_e = 1/2$, this potential well is described by the approximate expression

$$U(z) \approx \frac{15}{22}\hbar\gamma\frac{G\gamma^3}{|\delta|^3}\frac{k}{z_m}z^2 + \frac{15}{88}\hbar\gamma\frac{G^2\gamma^3}{|\delta|^3}kz_m \times \ln\left(1 + \frac{176}{51}\left(\frac{\delta}{G\gamma}\right)^2\left(\frac{z}{z_m}\right)^2\right), \tag{31}$$

where we introduced the characteristic length on which the Zeeman shift frequency is equal to the natural line width,

$$z_m = \frac{\hbar\gamma}{\mu_B a}. \tag{32}$$

The shape of the potential well (31) near the bottom is determined by the two-photon sub-Doppler resonance and its wings are determined by the Doppler resonance (Fig. 5). At the magnetic field gradient $a = 10$ G cm^{-1}, the characteristic length for the transition in ^{85}Rb with the natural line halfwidth $\gamma/2\pi = 2.95$ MHz under consideration is $z_m \approx 2.1$ mm.

The atomic oscillation frequency near the bottom of the potential well where the sub-Doppler resonance is effective is

$$\omega_v = \left(\frac{\gamma}{|\delta|}\right)^{1/2}\sqrt{\frac{40}{17}\frac{\lambda}{2\pi z_m}\gamma\omega_r}, \tag{33}$$

where $\omega_r = \hbar k^2/2M$ is the recoil frequency. At the same detunings $\delta = -10\gamma$ and the magnetic field gradient a = 10 G cm^{-1}, the oscillation frequency for the chosen transition with the characteristic recoil frequency $\omega_r/2\pi$ = 3.8 kHz is $\omega_v \approx 400$ Hz.

Let us now estimate the parameters of the compressed atomic beam. For a negative detuning ($\delta < 0$), radiation force (25) reduces to the frictional force

$$F = -M\beta v$$

with the coefficient of friction β, which at large detunings ($|\delta| \gg \gamma, \Omega$) is proportional to the recoil frequency:

$$\beta = \frac{120}{17}\frac{\gamma}{|\delta|}\omega_r. \quad (34)$$

The velocity dependence of the momentum diffusion tensor also includes the two-photon sub-Doppler resonance localized at zero velocity. For our purposes, it will suffice to use the diffusion coefficient D_{zz} at zero velocity and zero coordinate, $D_0 = D_{zz}(0, 0)$. This value of the diffusion coefficient, together with the coefficient of friction β, determines the atomic temperature near the quadrupole configuration axis according to the steady-state solution of the Fokker–Planck equation:

$$T = \frac{D_0}{M\beta}.$$

At large detunings ($|\delta| \gg \gamma, \Omega$), the momentum diffusion coefficient D_0 is estimated as

$$D_0 = \frac{23}{17}\hbar^2 k^2 \gamma \frac{G\gamma^2}{\delta^2}. \quad (35)$$

Accordingly, the transverse velocity distribution of the atomic beam near the quadrupole configuration axis is described by the Maxwellian distribution with the characteristic temperature

$$T = \frac{D_0}{M\beta} = \frac{23}{60}\frac{\hbar\gamma}{k_B}\frac{G\gamma}{|\delta|}. \quad (36)$$

The spatial distribution is described by the Boltzmann distribution

$$W(z) = \text{const} \cdot \exp\left(-\frac{U(z)}{k_B T}\right). \quad (37)$$

Since the potential has the form (31), the beam size near the bottom of the potential well depends only on the saturation parameter G and on the characteristic length z_m. For the chosen Lande factors, the beam width is estimated as

$$\Delta z = \sqrt{8k_B T/M\omega_v^2} = \sqrt{\frac{391}{150}G\frac{\lambda z_m}{2\pi}}. \quad (38)$$

For detuning $\delta = -10\gamma$, saturation parameter G = 0.5, and magnetic field gradient a = 10 G cm^{-1}, the temperature is 3 μK and the beam size is 18 μm.

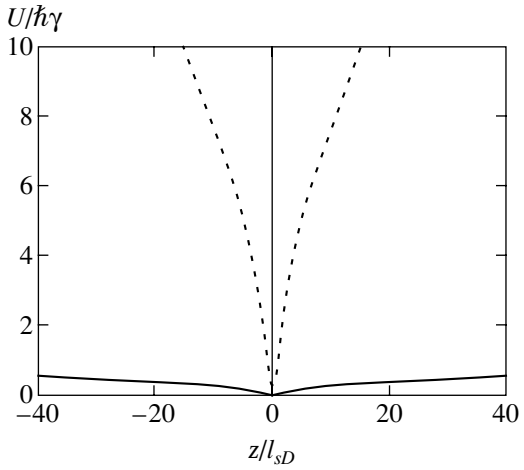

Fig. 5. The potential well for an atom at the same parameters as in Fig. 4.

It should be particularly emphasized that the above estimates are also retained for the beam compression along any other direction. Thus, in describing the compression of an atomic beam along the y axis, substituting the laser field (2) for field (3) in the basic equations does not change the above estimates. The estimates of the compression for any other directions include additional geometrical factors on the order of unity.

The widths of the velocity and spatial distributions determined above can be used to estimate the phase density of the compressed atomic beam. We give an estimate of the dimensionless phase density [22]:

$$\Lambda = \frac{N_a h^3}{(\Delta r \Delta p)^3}, \quad (39)$$

where N_a is the number of atoms in the beam and $(\Delta r \Delta p)^3$ is the phase volume occupied by the atoms. In the case of an atomic beam, it is convenient to express the phase density in terms of the mean atomic density n_a and to separate out the widths of the atomic momentum distribution along, Δp_l, and across, Δp_{tr}, the beam axis:

$$\Lambda = \frac{n_a h^3}{\Delta p_l (\Delta p_{tr})^2}. \quad (40)$$

The atomic density in the magnetic system under consideration is limited by the dipole–dipole atomic interaction, by the repulsive potential produced by scattered laser radiation, and by the attractive potential produced by the absorption of laser radiation. All these factors were studied in reasonable detail, because they play an important role in magnetooptical traps [23–26]. The most important factor is the reabsorption of photons inside the atomic ensemble. Multiple photon reabsorption causes the frictional and compressing forces to

decrease. A characteristic feature of an axisymmetric magnetic system is its small cross section. This circumstance shows that the atomic medium can remain optically transparent in the transverse direction at a relatively high density. A standard estimate for the atomic density $n_a = 1/\sigma\Delta z$ (where σ is the resonance absorption cross section) and available data on the atomic density in magnetooptical traps show that the maximum atomic density in the beam is limited to a value on the order of $n_a = 10^{12}$ cm^{-3}. If we take the realistic Doppler value of $\Delta p_l = M\gamma/k$ for the width of the longitudinal momentum distribution and the sub-Doppler value that corresponds to the temperature of 3 μK for the width of the transverse momentum distribution, we then obtain $\Lambda = 5 \times 10^{-4}$ for the ^{85}Rb atomic beam phase density.

7. CONCLUSION

Our analysis shows that the sub-Doppler resonances in the radiation force allow atomic beams to be compressed to values on the order of several tens of microns. Such a significant compression is, naturally, possible for slow atomic beams where the time of flight of the atoms is enough for the atomic temperature to be reduced to the sub-Doppler value.

Thus, we found that an atomic beam in a nonuniform magnetic field could be compressed to a diameter on the order of several tens of microns and the phase density could be increased to a value on the order of 10^{-4}–10^{-3}. Such a high expected atomic phase density in the compressed beam enables the subsequent evaporative cooling of the atoms down to quantum degeneracy for a realistic length of the magnetic trapping system [27]. In turn, the realization of this possibility may allow a continuous-wave atomic laser to be produced.

APPENDIX A

Below, we give the system of equations that defines the steady-state values of the functions $R^0_{g_\alpha g_\alpha} = N_\alpha$, $R^0_{e_\alpha e_\alpha} = n_\alpha$, and $S^0_{ab} = c_{ab}$:

$$\sum N_\alpha + \sum n_\alpha = 1, \tag{A.1}$$

$$i\Omega(c_{e_{-2}g_{-1}} - c_{g_{-1}e_{-2}}) + \frac{i\Omega}{\sqrt{6}}(c_{e_0g_{-1}} - c_{g_{-1}e_0}) + \gamma\left(2n_{-2} + n_{-1} + \frac{1}{3}n_0\right) = 0,$$

$$\frac{i\Omega}{\sqrt{2}}(c_{e_{-1}g_0} - c_{g_0e_{-1}} + c_{e_1g_0} - c_{g_0e_1}) + \gamma\left(n_{-1} + \frac{4}{3}n_0 + n_1\right) = 0,$$

$$i\Omega(c_{e_2g_1} - c_{g_1e_2}) + \frac{i\Omega}{\sqrt{6}}(c_{e_0g_1} - c_{g_1e_0}) + \gamma\left(\frac{1}{3}n_0 + n_1 + 2n_2\right) = 0,$$

$$i\Omega(c_{g_{-1}e_{-2}} - c_{e_{-2}g_{-1}}) - 2\gamma n_{-2} = 0,$$

$$\frac{i\Omega}{\sqrt{2}}(c_{g_0e_{-1}} - c_{e_{-1}g_0}) - 2\gamma n_{-1} = 0,$$

$$\frac{i\Omega}{\sqrt{6}}(c_{g_{-1}e_0} - c_{e_0g_{-1}} + c_{g_1e_0} - c_{e_0g_1}) - 2\gamma n_0 = 0,$$

$$\frac{i\Omega}{\sqrt{2}}(c_{g_0e_1} - c_{e_1g_0}) - 2\gamma n_1 = 0,$$

$$i\Omega(c_{g_1e_2} - c_{e_2g_1}) - 2\gamma n_2 = 0,$$

$$i\Omega(n_{-2} - N_{-1}) - (\gamma + i(\delta_1 - \omega_g + 2\omega_e))c_{g_{-1}e_{-2}} = 0,$$

$$\frac{i\Omega}{\sqrt{6}}(N_{-1} + c_{g_{-1}g_1} - n_0) + (\gamma + i(\delta_{-1} - \omega_g))c_{g_{-1}e_0} = 0,$$

$$\frac{i\Omega}{\sqrt{2}}(N_0 - n_{-1}) + (\gamma + i(\delta_1 + \omega_e))c_{g_0e_{-1}} = 0,$$

$$\frac{i\Omega}{\sqrt{2}}(N_0 - n_1) + (\gamma + i(\delta_{-1} - \omega_e))c_{g_0e_1} = 0,$$

$$\frac{i\Omega}{\sqrt{6}}(N_1 + c_{g_1g_{-1}} - n_0) + (\gamma + i(\delta_1 + \omega_g))c_{g_1e_0} = 0,$$

$$i\Omega(N_1 - n_2) + (\gamma + i(\delta_{-1} + \omega_g - 2\omega_e))c_{g_1e_2} = 0,$$

$$\frac{i\Omega}{\sqrt{6}}(c_{e_0g_1} - c_{g_{-1}e_0}) + 2i(\omega_g + kv)c_{g_{-1}g_1} = 0. \tag{A.2}$$

Equations (A.2) were derived from Eqs. (9) considered in the zero order in photon momentum. Normalization condition (17) was written as the first equation of system (A.1).

APPENDIX B

Below, we give the system of equations for the functions $Q^1_{g_\alpha g_\alpha} = Q_\alpha$, $Q^1_{e_\alpha e_\alpha} = q_\alpha$, and $T^1_{ab} = t_{ab}$:

$$\sum Q_\alpha + \sum q_\alpha = 0, \tag{B.1}$$

$$i\Omega(t_{e_{-2}g_{-1}} - t_{g_{-1}e_{-2}}) + \frac{i\Omega}{\sqrt{6}}(t_{e_0g_{-1}} - t_{g_{-1}e_0})$$
$$+ \gamma\left(2q_{-2} + q_{-1} + \frac{1}{3}q_0\right) = i\Omega(c_{e_{-2}g_{-1}} - c_{g_{-1}e_{-2}})$$
$$-\frac{i\Omega}{\sqrt{6}}(c_{e_0g_{-1}} - c_{g_{-1}e_0}) - fN_{-1},$$

$$\frac{i\Omega}{\sqrt{2}}(t_{e_{-1}g_0} - t_{g_0e_{-1}} + t_{e_1g_0} - t_{g_0e_1}) + \gamma\left(q_{-1} + \frac{4}{3}q_0 + q_1\right)$$
$$= \frac{i\Omega}{\sqrt{2}}(c_{e_{-1}g_0} - c_{g_0e_{-1}} - c_{e_1g_0} + c_{g_0e_1}) - fN_0,$$

$$i\Omega(t_{e_2g_1} - t_{g_1e_2}) + \frac{i\Omega}{\sqrt{6}}(t_{e_0g_1} - t_{g_1e_0}) + \gamma\left(\frac{1}{3}q_0 + q_1 + 2q_2\right)$$
$$= i\Omega(c_{g_1e_2} - c_{e_2g_1}) + \frac{i\Omega}{\sqrt{6}}(c_{e_0g_1} - c_{g_1e_0}) - fN_1,$$

$$i\Omega(t_{g_{-1}e_{-2}} - t_{e_{-2}g_{-1}}) - 2\gamma q_{-2}$$
$$= i\Omega(c_{e_{-2}g_{-1}} - c_{g_{-1}e_{-2}}) - fn_{-2},$$

$$\frac{i\Omega}{\sqrt{2}}(t_{g_0e_{-1}} - t_{e_{-1}g_0}) - 2\gamma q_{-1} = \frac{i\Omega}{\sqrt{2}}(c_{e_{-1}g_0} - c_{g_0e_{-1}}) - fn_{-1},$$

$$\frac{i\Omega}{\sqrt{6}}(t_{g_{-1}e_0} - t_{e_0g_{-1}} + t_{g_1e_0} - t_{e_0g_1}) - 2\gamma q_0 \qquad \text{(B.2)}$$
$$= \frac{i\Omega}{\sqrt{6}}(c_{g_{-1}e_0} - c_{e_0g_{-1}} - c_{g_1e_0} + c_{e_0g_1}) - fn_0,$$

$$\frac{i\Omega}{\sqrt{2}}(t_{g_0e_1} - t_{e_1g_0}) - 2\gamma q_1 = \frac{i\Omega}{\sqrt{2}}(c_{g_0e_1} - c_{e_1g_0}) - fn_1,$$

$$i\Omega(t_{g_1e_2} - t_{e_2g_1}) - 2\gamma q_2 = i\Omega(c_{g_1e_2} - c_{e_2g_1}) - fn_2,$$

$$i\Omega(q_{-2} - Q_{-1}) - (\gamma + i(\delta_1 - \omega_g + 2\omega_e))t_{g_{-1}e_{-2}}$$
$$= i\Omega(N_{-1} + n_{-2}) - fc_{g_{-1}e_{-2}},$$

$$\frac{i\Omega}{\sqrt{6}}(Q_{-1} - q_0 + t_{g_{-1}g_1}) + (\gamma + i(\delta_{-1} - \omega_g))t_{g_{-1}e_0}$$
$$= \frac{i\Omega}{\sqrt{6}}(N_{-1} + n_0 - c_{g_{-1}g_1}) + fc_{g_{-1}e_0},$$

$$\frac{i\Omega}{\sqrt{2}}(q_{-1} - Q_0) - (\gamma + i(\delta_1 + \omega_e))t_{g_0e_{-1}}$$
$$= \frac{i\Omega}{\sqrt{2}}(N_0 + n_{-1}) - fc_{g_0e_{-1}},$$

$$\frac{i\Omega}{\sqrt{2}}(q_1 - Q_0) - (\gamma + i(\delta_{-1} - \omega_e))t_{g_0e_1}$$
$$= -\frac{i\Omega}{\sqrt{2}}(N_0 + n_1) - fc_{g_0e_1},$$

$$\frac{i\Omega}{\sqrt{6}}(q_0 - Q_1 - t_{g_1g_{-1}}) - (\gamma + i(\delta_1 + \omega_g))t_{g_1e_0}$$
$$= \frac{i\Omega}{\sqrt{6}}(N_1 + n_0 - c_{g_1g_{-1}}) - fc_{g_1e_0},$$

$$i\Omega(q_2 - Q_1) - (\gamma + i(\delta_{-1} + \omega_g - 2\omega_e))t_{g_1e_2}$$
$$= -i\Omega(N_1 + n_2) - fc_{g_1e_2},$$

$$\frac{i\Omega}{\sqrt{6}}(t_{e_0g_1} - t_{g_{-1}e_0}) + 2i(\omega_g + kv)t_{g_{-1}g_1}$$
$$= -\frac{i\Omega}{\sqrt{6}}(c_{e_0g_1} + c_{g_{-1}e_0}) - fc_{g_{-1}g_1}.$$

Equations (B.2) were derived from Eqs. (9) considered in the first order in photon momentum. The first equation of system (B.1) is normalization condition (19). The quantity $f = F/\hbar k\gamma$ is the normalized force.

ACKNOWLEDGMENTS

This study was supported in part by the Russian Foundation for Basic Research (project nos. 01-02-16337, 02-02-17014) and INTAS (grant no. 479).

REFERENCES

1. J. Nellessen, J. Werner, and W. Ertmer, Opt. Commun. **78**, 300 (1990).
2. M. Schiffer, M. Christ, G. Wokurka, and W. Ertmer, Opt. Commun. **134**, 423 (1997).
3. W. Ketterle and N. J. van Druten, in *Advances in Atomic, Molecular and Optical Physics*, Ed. by B. Bederson and H. Walther (Academic, San Diego, 1996), Vol. 37, p. 181.
4. J. T. M. Walraven, in *Quantum Dynamics of Simple Systems*, Ed. by G. L. Oppo and S. M. Barnett (Institute of Physics, London, 1996), p. 315.
5. G. Nienhuis, P. van der Straten, and S.-Q. Shang, Phys. Rev. A **44**, 462 (1991).
6. M. Walhout, J. Dalibard, S. L. Rolston, and W. D. Phillips, J. Opt. Soc. Am. B **9**, 1997 (1992).
7. J. Werner, H. Wallis, and W. Ertmer, Opt. Commun. **94**, 525 (1992).
8. P. van der Straten, S.-Q. Shang, B. Sheehy, *et al.*, Phys. Rev. A **47**, 4160 (1993).
9. C. Valentin, M.-C. Gagne, J. Yu, and P. Pillet, Europhys. Lett. **17**, 133 (1992).
10. M. Walhout, U. Sterr, and S. L. Rolston, Phys. Rev. A **54**, 2275 (1996).
11. S. Weyers, E. Aucouturier, C. Valentin, and N. Dimarcq, Opt. Commun. **143**, 30 (1997).

12. P. Berthoud, A. Joyet, G. Dudle, *et al.*, Europhys. Lett. **41**, 141 (1998).
13. Y. Fukuyama, H. Kanou, V. I. Balykin, and K. Shimizu, Appl. Phys. B **70**, 561 (2000).
14. S.-Q. Shang, B. Sheehy, P. van der Straten, and H. Metcalf, Phys. Rev. Lett. **65**, 317 (1990).
15. S.-Q. Shang, B. Sheehy, P. van der Straten, *et al.*, Phys. Rev. Lett. **67**, 1094 (1991).
16. R. Golub and J. M. Pendlebury, Rep. Prog. Phys. **42**, 439 (1979).
17. S. G. Rautian, G. I. Smirnov, and A. M. Shalagin, *Nonlinear Resonances in Atomic and Molecular Spectra* (Nauka, Novosibirsk, 1979).
18. S. Chang and V. Minogin, Phys. Rep. **365/2**, 65 (2002).
19. V. G. Minogin and V. S. Letokhov, *Laser Light Pressure on Atoms* (Gordon and Breach, New York, 1987).
20. S. Chang, T. Y. Kwon, Ho S. Lee, and V. Minogin, Phys. Rev. A **60**, 2308 (1999).
21. S. Chang, T. Y. Kwon, Ho S. Lee, and V. G. Minogin, Phys. Rev. A **60**, 3148 (1999).
22. F. Lison, P. Schuh, D. Haubrich, and D. Meshede, Phys. Rev. A **61**, 013405 (1999).
23. D. W. Sesko, T. G. Walker, and C. E. Wieman, J. Opt. Soc. Am. B **8**, 946 (1991).
24. A. M. Steane, M. Chowdhurry, and C. J. Foot, J. Opt. Soc. Am. B **9**, 2142 (1992).
25. M. Drewsen, P. Laurent, A. Nadir, *et al.*, Appl. Phys. B **59**, 283 (1994).
26. C. G. Townsend, N. H. Edwards, C. J. Cooper, *et al.*, Phys. Rev. A **52**, 1423 (1995).
27. E. Mandonnet, A. Minguzzi, R. Dum, *et al.*, Eur. Phys. J. D **10**, 9 (2000).

Translated by V. Astakhov